Full Paper

J. Agric. Meteorol. 69 (1): 23-32, 2013

Proposal of a new equation to estimate globe temperature in an urban park environment

Maki OKADA*, †, and Hiroyuki KUSAKA**

*Graduate School of Life and Environmental Sciences, University of Tsukuba, 1-1-1 Tennodai, Tsukuba, Ibaraki, 305-8572, Japan

**Center for Computational Sciences, University of Tsukuba, 1-1-1 Tennodai, Tsukuba, Ibaraki, 305-8577, Japan

Abstract

Globe temperature is one element of the heat stress index, the Wet Bulb Globe Temperature, which is used to evaluate how radiation adds to thermal discomfort in the workplace. As the measurement of globe temperature is not standardized, empirical equations were introduced to estimate the globe temperature from weather factors, including air temperature, solar radiation and wind speed. As it was not known whether these equations were applicable in an urban park environment with vegetation, we observed the globe temperature using a set of instruments in three parks. The observation along with the heat balance analysis of the globe revealed that the globe temperature depended curvilinearly on solar radiation and that wind speed influenced this dependence. We compared two previously proposed empirical equations to the observed globe temperature and found both equations had systematic estimation errors. Although the errors were reduced by fitting the equations to the observed data and reevaluating their numerical constants, the equations still had shortcomings, as one did not consider wind speed and the other included a discontinuity. We therefore derived a new equation based on the heat balance equations of the globe with its numerical constants experimentally determined. This equation was able to predict the curvilinear dependence of the globe temperature on global solar radiation without any discontinuity, and it also showed the globe temperature response to wind speed.

Key words: Empirical equation, Globe temperature, Ground surface condition, Heat balance, WBGT, Wet bulb globe temperature.

1. Introduction

Thermal indices have been introduced to predict the risk of heat stress on human health in environments where humans exercise. Among them, the Wet Bulb Globe Temperature (WBGT: Yaglou and Minard, 1957) is a thermal index developed more than 50 years ago that has been recognized as a standard heat stress index by public agencies worldwide (Budd, 2008; ISO7243, 1989; JIS Z 8504, 1999; Japanese Ministry of the Environment, 2011). Calculation of the WBGT index requires measurement of three parameters: the natural wet bulb temperature, the globe temperature, and the air temperature. Because the first two parameters are not typically recorded by the Japanese network of meteorological stations, direct evaluation of the WBGT index is not possible. Some empirical equations have been proposed to predict the WBGT index or its parameters from generally observed weather variables such as air temperature, humidity, wind speed and solar radiation (Nakai *et al*., 1992; Takaichi *et al*., 2003; Ono *et al*., 2006; Tonouchi and Murayama, 2008). Horie and Fujiwara (2010) evaluated the accuracy of these four equations in comparison with WBGT parameters measured on their building roof, and concluded that the errors of estimation were minimized when the globe temperature calculated by the formula proposed by Tonouchi and Murayama (2008) was used to predict the WBGT.

Although the WBGT thermal index thus calculated gives criteria to avoid the risk of heat stress, it is not known whether the index can be applied to environ-

Received; May 23, 2012.

Accepted; December 26, 2012.

† Corresponding Author: mokada@geoenv.tsukuba.ac.jp

ments having surfaces different from where the equations were experimentally derived and their numerical constants were determined. In particular, the environment of an urban park with vegetation is different from that in surrounding city zones.

Park environments play an important role in mitigating the effects of an urban heat island and the thermal discomfort felt in its vicinity (Eliasson and Upmanis, 2000; Nagatani *et al*., 2008), and their climate itself invites people to a park for leisure or exercise. It has, however, not been discussed whether the standard empirical equations used to estimate the globe temperature for predicting the WBGT index could be applied to an urban park environment. Changes in wind regime and/or surrounding ground temperature would affect the globe temperature through convection and long-wave radiation exchange.

In this study we observed the globe temperature and weather factors in three parks and investigated the response of the globe temperature to the weather factors by heat balance analysis of the globe. We then examined two previously proposed empirical equations (Takaichi *et al*., 2003; Tonouchi and Murayama, 2008) and discussed reasons for disagreement between the predictions using these equations and the observations. Finally we proposed a new equation based on heat balance equations of the globe to predict the globe surface temperature.

2. Materials and Methods

2.1 Measurement of globe temperature and weather variables

We conducted the experiment from 8 to 10 September 2011 at three parks, each of a different size, in the city of Tsukuba: Doho park (20 ha), Ninomiya park (4 ha) and Kitamukai park (0.5 ha). Air temperature and relative humidity were measured with a thermistor sensor RTR-52A and RTR-53A (T&D, Matsumoto, Japan) installed in an aspirated radiation shield (Murakami and Kimura, 2010). Globe temperature was measured with an RTR-52A thermistor inserted in a Vernon type globe with a diameter of 150 mm. Solar radiation and wind speed were measured using the weather station system "Vantage Pro2" (Davis Instruments, San Francisco, USA) with a solar radiation sensor and a cup anemometer. Each instrument was placed at a height of 1.5 m above open sunlit turf grass in each park. The recording interval was 5 seconds for air and globe temperature and relative humidity, but 1 minute for wind speed and 10 minutes for solar radiation because of the restrictions of the data logging procedure. In general, a 10-minute interval is too long to accurately measure variable solar radiation, so we did not use the instantaneous record, but three consecutive records at 10-minute intervals collected when solar radiation was continuously stable. A 20-minute mean value was calculated from the three records by assuming a linear change between two adjacent records. Accordingly, all of the other variables were averaged over 20 minutes.

2.2 Calculation of the heat balance of the globe and the surrounding ground surface

We assume that the globe is placed above an open flat surface where the globe can view only the sky and the ground. The variables, which are not explained below, are compiled on a list of symbols.

Heat balance at the globe surface is given by:

$$S + L + H = 0 \qquad (1)$$

where S is short-wave radiation flux, L is long-wave radiation flux and H is convective heat flux.

By reference to previous studies (Toriyama *et al*., 2001; Ohashi *et al*., 2009; Gaspar and Quintela, 2009), short-wave radiation flux S on the globe surface is given by the sum of three components, namely, the direct beam from the sun, diffuse radiation from the sky and the reflection of short-wave radiation from below (Eq. (2)):

$$S = \alpha_g \left(\frac{S_{nor}}{4} + \frac{S_{dif}}{2} + \frac{S_{ref}}{2} \right) \qquad (2)$$

Note that the flux density of S_{nor} is based on the surface perpendicular to the solar beam, whereas S_{dif} and S_{ref} are based on a horizontal surface. The constant in the denominator of the first term in the parentheses results from the ratio of the projected globe area perpendicular to the direct solar beam (πr^2) to the surface of the globe ($4\pi r^2$) and the constants in the denominator of the last two terms from the view factor of the globe surface relative to the sky and that to the ground surface, respectively. When the global solar radiation S_o at the horizontal surface and the albedo a_l of the surrounding ground surface are used instead of S_{nor} and S_{ref}, Eq. (2) is rewritten as:

$$S = \alpha_g \left(\frac{S_o - S_{dif}}{4\cos\theta} + \frac{S_{dif}}{2} + \frac{a_l S_o}{2} \right) \qquad (3)$$

Long-wave radiation flux L on the globe surface is given by Eq. (4). Again, the constants in the denominator correspond respectively to the view factor of the globe relative to the sky and to the ground.

$$L = \varepsilon_g \left(\frac{L_{sky}}{2} + \frac{\varepsilon_{gr} \sigma T_{gr}^4}{2} - \sigma T_g^4 \right) \quad (4)$$

Convective heat flux H in Eq. (1) at the globe surface is given by Eq. (5):

$$H_g = \rho c_p C_H U \left(T_a - T_g \right) \quad (5)$$

The bulk coefficient of the globe C_H in Eq. (5) is calculated from the empirical form proposed by Toriyama *et al*. (2001):

$$C_H = 0.0156 U^{-0.82} \quad (6)$$

In order to calculate Eq. (4), the surrounding ground surface temperature T_{gr} is required. The heat balance at the ground surface is given by:

$$\left(1 - a_l\right) S_o + \varepsilon_{gr} \left(L_{sky} - \sigma T_{gr}^4 \right) = H_{gr} + lE + G \quad (7)$$

where lE is latent heat flux and G is ground heat flux.

By introducing the Bowen ratio β and assuming that the heat flux G into the soil is 30% of the net radiation at the ground surface (Oke, 1987), Eq. (7) can be rewritten as follows:

$$0.7 \left\{ \left(1 - a_l\right) S_o + \varepsilon_{gr} \left(L_{sky} - \sigma T_{gr}^4 \right) \right\} - H_{gr} - \frac{H_{gr}}{\beta} = 0 \quad (8)$$

Convective heat flux H_{gr} in Eq. (8) is calculated using a bulk transfer equation.

$$H_{gr} = \rho c_p C_H^* U \left(T_{gr} - T_a \right) \quad (9)$$

C^*_H in Eq. (9) is a transport coefficient for a grass field with a plant height of 0.1 m in calm and unstable conditions (Kondo, 2000).

$$C_H^* = 0.0065 \left(T_{gr} - T_a \right)^{1/3} \quad (10)$$

Equation (10) can be applied to wind speeds below 2.0 m s^{-1}. In this study, the observed mean wind speed was 0.57 m s^{-1}, the maximum wind speed was 1.3 m s^{-1}, and no measurement exceeded 2.0 m s^{-1}.

2.3 Weather variables and parameters used in the model calculation

Diffuse solar radiation S_{dif} is required to calculate Eq. (3), but no diffuse solar radiation was measured in the experiment. We first calculated both direct and diffuse solar radiation for a clear sky from Eqs (11) and (12) given by Campbell and Norman (1998) using 1365 W m^{-2} for the solar constant and 0.7 for atmospheric transmittance. We then estimated the diffuse solar radiation by multiplying the observed global solar radiation by the ratio of S_{dif} to the sum of S_d and S_{dif} calculated from the following equations.

$$S_d = S_{po} \tau^m \cos\theta \quad (11)$$

$$S_{dif} = 0.3 \left(1 - \tau^m\right) S_{po} \cos\theta \quad (12)$$

The solar zenith angle for the experimental place and time was obtained from the website of the Ephemeris Computation Office, Public Relations Center, National Astronomical Observatory of Japan (http://eco.mtk.nao.ac.jp/koyomi/index.html).

Long-wave sky radiation L_{sky} in Eq. (4) is calculated from Brunt's equation (Brunt, 1939) with air temperature T_a and water vapor pressure e at ground level according to the parameters of Watanabe (1965):

$$L_{sky} = \left(0.52 + 0.063\sqrt{e}\right) \sigma T_a^4 \quad (13)$$

In the model calculation, the values of 0.92 and 0.95 were used for the absorptivity (Toriyama *et al*., 2001) and the emissivity (Ohashi *et al*., 2009) of the globe surface, respectively. The albedo and the emissivity of the surrounding ground used 0.2 (Munn, 1966) and 0.95 by assuming a grass surface.

3. Results and Discussion

3.1 Verification of the heat balance model of the globe

For comparison with the observations, the globe and the surrounding ground surface temperature were calculated by giving air temperature, humidity, solar radiation and wind speed observed in the experiment. The Bowen ratio was introduced to simulate the change in wetness and resultant surface temperature of the surrounding ground in the heat balance model. As we did not observe the Bowen ratio in the experiment, we first determined the Bowen ratio so as to minimize errors in estimating the globe temperature by the model. The root mean square error (RMSE) of estimation became the smallest at a Bowen ratio of 1.1. The Bowen ratio thus determined corresponds to that obtained on a dry grass surface in the previous studies (*e.g.* Inoue *et al*., 2004). Our experiment sites were covered with turf

grass, which had often been mowed but not artificially irrigated. At the time of the experiment the grass surface was dry so that the value of 1.1 is considered to be in a reasonable range of the Bowen ratio in this study.

The predicted globe temperature by the heat balance model was compared to that observed in Fig. 1 where RMSE was at its minimum of 1.2℃ at the Bowen ratio of 1.1. Figure 1 indicates that the heat balance model developed here can properly simulate the response of the globe temperature to weather variables in three different parks and the site-specific deviation of prediction errors across the experiment sites was not significant.

3.2 Dependence of globe temperature on weather conditions and ground surface temperature

Previously proposed empirical equations were derived from observations in a dry greenhouse（Takaichi *et al*., 2003）or on the roof of a building（Tonouchi and Murayama, 2008）, whereas our data were collected in green parks. One can speculate that wind conditions and/or the surrounding ground surface temperature would differ among these sites and thus would affect the globe temperature through convection and exchange of long-wave radiation. To evaluate the effects of wind and surrounding ground surface conditions, we conducted the analysis using the heat balance model.

Suppose that the globe is similarly exposed to wind and sunlight in an open space, whether in a park or on a building roof. In the model calculation, air temperature was fixed at the mean value of 30.3℃ averaged over the observed data from 27.6 to 33.3℃, and water vapor pressure was also fixed at the mean value of 23.1 hPa averaged over the observed data from 13.5 to 30.0 hPa and the Bowen ratio at 1.1 as determined above. Direct and diffuse solar radiation was calculated from Eqs（11）and（12）by changing the solar zenith angle under an assumed clear sky.

Since the globe temperature largely depends not only on solar radiation and/or wind speed but also on air temperature, we plotted the globe minus air temperature difference（T_g−T_a）as a function of solar radiation（Fig. 2）. The observed T_g−T_a is shown separately for wind speed ranges above and below 0.5 m s^{-1} in Fig. 2. The calculated T_g−T_a by the heat balance model was also plotted in the same figure for a wind speed of 0.2, 0.57 and 1.3 m s^{-1}; each corresponding to the minimum, mean and maximum wind speed observed in the experiment.

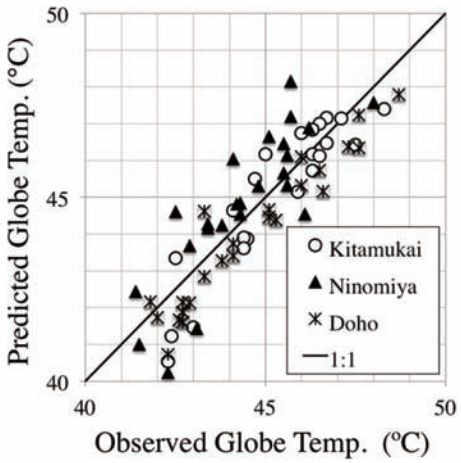

Fig. 1. Comparison of the globe temperature predicted by the physical model to that observed. Symbols denote the data observed in three different parks. The globe temperature is predicted by using the observed air temperature, solar radiation, wind speed and water vapor pressure as input variables and the Bowen ratio fixed at 1.1.

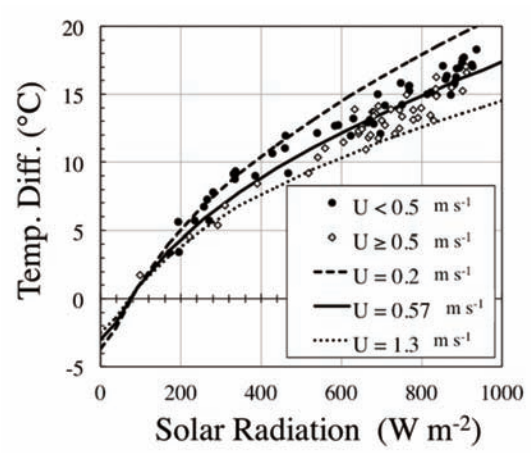

Fig. 2. Effects of wind speed on the relationship between the temperature difference（T_g−T_a）and global solar radiation calculated by the physical model. The Bowen ratio is fixed at 1.1. The black dots indicate the observed data for a wind speed range below 0.5 m s^{-1} and the open diamonds above 0.5 m s^{-1}.

Both the observed and the calculated T_g-T_a similarly responded to the change in solar radiation curvilinearly. As represented in Eq. (3), the curvilinear response of T_g-T_a to solar radiation results from the term that includes the cosine of the solar zenith angle θ. This response is considered to be significant as a behavior of the globe temperature in relation to solar radiation.

The observed T_g-T_a in Fig. 2 tended to increase as wind speed decreased and suggests that wind speed had an influence on the curvilinear response to solar radiation. The influence of wind speed was more clearly explained by the model calculation. The variation induced by changes in wind speed became large as the solar radiation increased.

We then evaluated the effect of the surrounding ground surface temperature on the globe temperature by altering the Bowen ratio in the range between 0.2 for well-watered turf grass (Kondo, 1994) and 5.0 for an asphalt surface (Kondo, 1994). Figure 3 shows the temperature difference (T_g-T_a) calculated for three levels of the Bowen ratio at a wind speed of 0.2 m s^{-1}, the observed minimum (top) and of 0.57 m s^{-1}, the observed mean (bottom). At a larger wind speed the curves were similar to those in Fig. 3, but T_g-T_a decreased and the distance between the curves became closer (data not shown).

The globe temperature depended on the surrounding ground surface temperature, especially when the solar radiation was intense, and the globe temperature increased as the Bowen ratio became larger (Fig. 3). For example the globe and the ground surface temperature calculated by the model was 44.3℃ and 41.2℃ at a Bowen ratio of 0.2, 46.4℃ and 55.3℃ at 1.0, and 47.5℃ and 62.0℃ at 5.0, respectively, when solar radiation was 900 W m^{-2} and wind speed 0.57 m s^{-1}. The increase of the globe temperature accompanied by an increased Bowen ratio, however, tended to diminish. As seen in Fig. 3, the distance between the curves for $\beta=0.2$ and $\beta=1.0$ was much larger than that between the curves for $\beta=1.0$ and $\beta=5.0$, and the curve for a Bowen ratio larger than 5.0 was close to the curve for 5.0 (data not shown). This means that the Bowen ratio, which measures the moisture of the surrounding ground surface, by itself cannot affect the globe temperature except a surface that is as wet as well-watered grass vegetation or water surface.

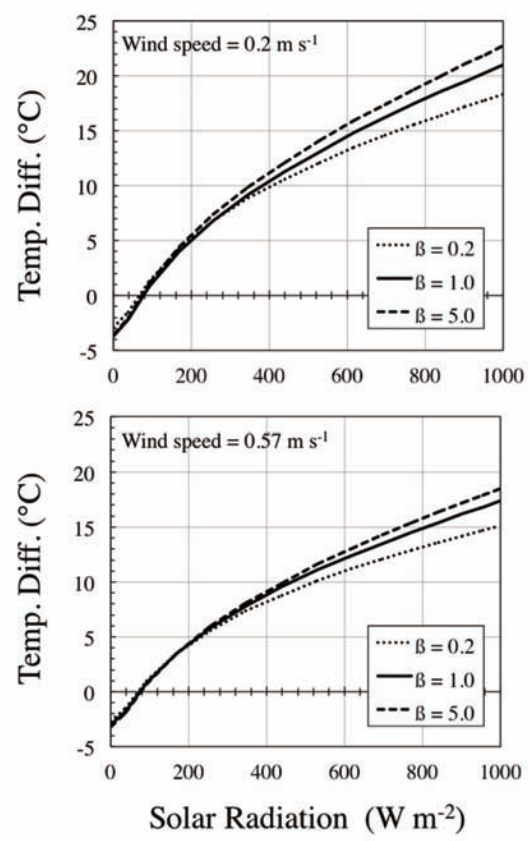

Fig. 3. Effects of the Bowen ratio of the surrounding ground surface on the relationship between the temperature difference (T_g-T_a) and global solar radiation calculated by the physical model; at a wind speed of 0.2 m s^{-1} (top) and at 0.57 m s^{-1} (bottom).

3.3 Applicability of the previous empirical equations

Following Horie and Fujiwara (2010), we investigated the following two empirical equations to estimate the globe temperature T_g:

$$T_g = T_a + 0.090 S_o / (1 + 0.0037 S_o) \qquad (14)$$

$$\begin{aligned} T_g &= T_a - 0.3 + 0.0256 S_o - 0.18 U^{1/2} \\ &\quad (S_o \le 400 W\, m^{-2}) \\ T_g &= T_a + 12.1 + 0.0067 S_o - 2.40 U^{1/2} \\ &\quad (S_o > 400 W\, m^{-2}) \end{aligned} \qquad (15)$$

Takaichi *et al.* (2003) proposed Eq. (14) to evaluate the occupational risk of greenhouse workers.

Tonouchi and Murayama (2008) proposed Eq. (15), and it is currently in use by the Ministry of the Environment to calculate the WBGT index with data from the Japanese national network of meteorological stations.

The observed globe minus air temperature difference ($T_g - T_a$) was plotted as a function of solar radiation in the three parks together with the functions given by the two empirical equations in Fig. 4a. Equation (15) was calculated for four wind speeds, 0, 0.57, 2 and 4 m s^{-1}. Equation (14) is a hyperbolic function of solar radiation and disregards wind speed. Equation (15) consists of two linear bivariate functions of solar radiation and wind speed; one is used for solar radiation above 400 W m^{-2} and the other for solar radiation below that value. The two functions are not contiguous at this boundary, and thus show a notable discontinuity especially at wind speeds near zero.

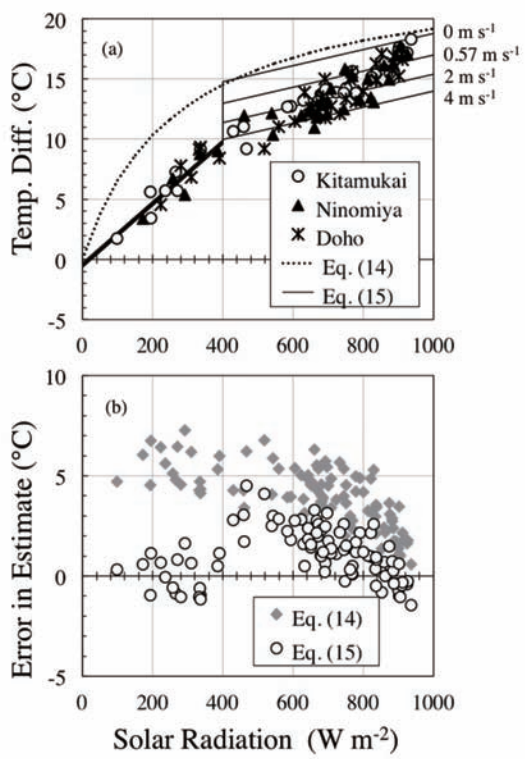

Fig. 4. (a) Dependence of the temperature difference ($T_g - T_a$) calculated from the two empirical equations on global solar radiation. Symbols denote the observed data in three different parks. The dotted line indicates the calculation by Eq. (14) and the solid lines by Eq. (15) at four wind speeds.
(b) Errors in estimate [estimated T_g from Eq. (14) or (15) minus measured T_g] as a function of global solar radiation.

Comparison of the estimates by the empirical equations with the observed values clearly showed systematic errors (Fig. 4b). The globe temperature was estimated by giving observed solar radiation, wind speed and air temperature to the empirical equations and the errors in the estimate [estimated T_g minus measured T_g] were plotted against solar radiation. Equation (14) overestimated the globe temperature over almost the entire range of solar radiation, especially at low radiation intensity. Horie and Fujiwara (2010) reported a similar result, although their location on a building roof was different thermally and environmentally from ours in a green park. Equation (15) also overestimated the globe temperature, but the error depended to a considerable extent on solar radiation: the errors were very small for solar radiation below 400 W m^{-2}, where the first formula in Eq. (15) was used. Above 400 W m^{-2}, where the second formula was used in Eq. (15), the errors decreased as solar radiation increased. Therefore, the errors were largest near the discontinuity where we switched from one formula to the other. As clearly seen in Fig. 4a, the slope of the second formula of Eq. (15) was different from that of the observations, whereas the slope of the first formula was quite similar to the slope of the observations.

We first hypothesized that the overestimation by Eqs. (14) and (15) was caused by site-specific differences in surrounding ground surface conditions such as surface moisture. The former model calculation, however, did not support this hypothesis, but it suggested that wind speed was more influential on the relationship between the globe temperature and solar radiation. One possible reason for the overestimation is, hence, the different wind regime at the measurement sites where the empirical equations and their numerical constants were derived. In fact, Eq. (14), which has no wind term, was derived in a greenhouse, and Eq. (15) was derived from observations made on a building roof. Wind conditions (especially turbulence) both in a greenhouse and on a building roof may be considerably different from those at ground level in a park. The numerical constants used in the empirical equations may therefore reflect a bias specific to the site where they were determined.

To determine values for the constants applicable to the urban park environment, we fitted the equations to the observed data. As Eq. (14) is a non-linear function of solar radiation, the downhill Simplex method, an optimization technique to search the minimum value of a nonlinear function, was used to determine the constants that minimized the sum of squared errors. Multiple regression was used to fit Eq. (15) to the data. The newly determined constants of Eqs. (14) and (15) are shown in Table 1. The errors in the new estimate were significantly improved (Fig. 5a and b): the root mean square error (RMSE) of Eq. (14) was reduced from 4.3℃ to 1.0℃, and RMSE of Eq. (15) was reduced from 1.6℃ to 0.76℃, after the numerical constants were altered.

The discontinuity in Eq. (15) became small but was not eliminated, since it is inherent in the form of the equations. $T_g - T_a$ calculated with Eq. (14) more closely followed the observed curvilinear response of the globe temperature to solar radiation, although it could not reflect differences related to wind speed.

3.4 Development of a new equation

As the analysis based on the heat balance of the globe revealed that the globe temperature depended curvilinearly on solar radiation and wind speed influenced this dependence, we derive a new equation to estimate the globe temperature by rearranging the equations of the physical model of the globe.

Eqs. (4) and (5) were substituted into Eq. (1):

$$S + L_a - \varepsilon_g \sigma T_g^4 + h_c \left(T_a - T_g\right) = 0 \qquad (16)$$

where $h_c = \rho c_p C_H U$, $L_a = \varepsilon_g \left(L_{sky} + \varepsilon_{gr} \sigma T_{gr}^4\right)/2$.

Equation (16) is rearranged with respect to the term $(T_g - T_a)$.

$$h_c \left(T_g - T_a\right) + \varepsilon_g \sigma \left(T_g^4 - T_a^4\right) = S + L_a - \varepsilon_g \sigma T_a^4 \qquad (17)$$

The nonlinear term $T_g^4 - T_a^4$ in Eq. (17) was linearized according to the Taylor expansion.

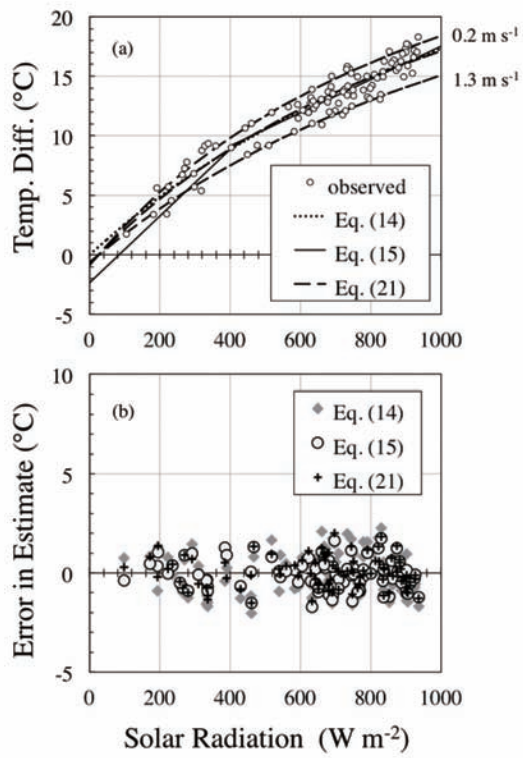

Fig. 5. (a) Dependence of the temperature difference $(T_g - T_a)$ calculated from the two empirical equations with newly determined numerical constants (see Table 1) and the new equation (21) on global solar radiation together with the observed values. Eqs. (14) and (15) are plotted for a wind speed of 0.57 m s^{-1}, and Eq. (21) for wind speeds of 0.2 and 1.3 m s^{-1}.
(b) Errors in estimate [estimated T_g minus measured T_g] given by the three equations.

$$\left(h_c + h_r\right)\left(T_g - T_a\right) = S + L_a - \varepsilon_g \sigma T_a^4 \qquad (18)$$

$$T_g = \left(S + L_a - \varepsilon_g \sigma T_a^4\right)/\left(h_c + h_r\right) + T_a \qquad (19)$$

where $h_r \approx 4 \varepsilon_g \sigma T_a^3$.

Suppose that h_c is a simple function of wind speed

Table 1. Empirical equations (14 and 15) with newly determined numerical constants and the newly proposed equation (21)

Eq. (14)	$T_g = T_a + 0.0271 S_o/(1 + 0.000563 S_o)$
Eq. (15)	$T_g = T_a + 0.557 + 0.0277 S_o - 2.39 U^{1/2}$ $(S_o \leq 400 W\ m^{-2})$ $T_g = T_a + 6.40 + 0.0142 S_o - 3.83 U^{1/2}$ $(S_o > 400 W\ m^{-2})$
Eq. (21)	$T_g = T_a + (S_o - 30.0)/(0.0252 S_o + 10.5 U + 25.5)$

(McAdams, 1954), that is, $h_c = k_1U + k_2$ and solar radiation and wind speed are only variables available for the inputs. Then Eq. (19) is reduced to the form:

$$T_g = (S + j_1)/(k_1U + j_2) + T_a \qquad (20)$$

where $j_1 = L_a - \varepsilon_g \sigma T_a^4$, $j_2 = k_2 + h_r$.

Since global solar radiation S_0 is the only variable obtainable from weather stations, S must be replaced with S_0. As suggested by Eq. (14) in Fig. 5a, a hyperbolic function adapts flexibly to the nonlinear response of the globe temperature to global solar radiation. We incorporated this idea and obtained the new empirical equation shown below:

$$T_g = (S_o + a)/(bS_o + cU + d) + T_a \qquad (21)$$

The numerical constants in Eq. (21) were determined as in Table 1 by fitting the equation to the observed data by the downhill Simplex method and the resulting curves are shown in Fig. 5a. $T_g - T_a$ calculated with Eq. (21) is able to respond nonlinearly to global solar radiation without any discontinuity and it also responds to wind, unlike $T_g - T_a$ calculated with Eq. (14), although the errors in the estimate were of a similar order among the three equations (Fig. 5b); the RMSE for Eq. (21) was 0.78℃. Equation (14) requires only two constants but cannot respond to changes in wind speed. Equation (15) requires totally six constants to respond to solar radiation and wind speed, while the new equation (21) requires four constants.

As mentioned in section 2.2, the observations were conducted under a limited range of wind speeds. Wind speed exceeded 1.0 m s^{-1} in only five of the 96 observations, and the maximum observed speed was 1.3 m s^{-1}. Thus, the numerical constants determined from those data can be applied to calm wind conditions under which severe heat stress is usually encountered, but may not be used for wind speed out of the experimental range (wind speed below 1.3 m s^{-1}).

4. Conclusion

We investigated the responses of the globe temperature on the weather conditions and the surrounding ground conditions as part of a study intended to evaluate heat stress on humans in environments where they exercise. Since the equations used were originally derived from observations made on a building roof or in a greenhouse, we examined whether they were applicable to an urban park environment. The two equations examined here overestimated the globe temperature experimentally observed in three urban parks. We first speculated that this overestimation was caused by differences in the condition of the surrounding ground, such as surface moisture, but an analysis of the heat balance of the globe did not support this speculation. The globe temperature did increase when the surrounding ground surface was dryer, but the increase was too low to account for the overestimation by the empirical equations. The heat balance analysis suggested that wind speed was more influential on the globe temperature and site-specific difference in wind regime caused the overestimation of the equations.

When we reevaluated the numerical constants in the empirical equations by fitting them to the observed data, the errors in estimate were largely reduced. There is bias in the constants of these equations, specific to the site where they were empirically determined, so the constants need to be reevaluated at each site where the model is applied. Although we reduced the errors by reevaluating the constants, there were still inherent defects in the formulas, including no effect of the wind and a discontinuity in the predicted nonlinear response to solar radiation.

Using our physical model of the globe, we then derived a new equation for the globe temperature that depends nonlinearly on global solar radiation without any discontinuity and takes into account wind speed. The numerical constants of the new equation were determined experimentally by fitting the equation to the data observed on the dry grass surface in the parks. Since the heat balance analysis of the globe revealed that the effect of the surrounding ground surface on the globe temperature is small except when the surface is very wet, our proposed new empirical equation is applicable to environments other than a green park.

Acknowledgments

We deeply appreciate the useful comments and suggestions of Prof. Masumi Okada at Iwate University. We also thank Prof. Hiroshi L. Tanaka for allowing us to use the meteorological instruments. The present study was supported by the Research Program on Climate Change Adaptation (RECCA) and by the Environment Research and Technology Development Fund (S-8) of the Ministry of the Environment, Japan.

Appendix

List of Symbols

a_l: albedo of the ground surface
c_p: specific heat of air at constant pressure (J K^{-1} kg^{-1})
C_H: bulk coefficient of the globe surface
C_H^*: bulk coefficient of the ground surface
e: atmospheric water vapor pressure (hPa)
E: evapotranspiration (kg m^{-2} s^{-1})
G: ground heat flux (W m^{-2})
h_c: convective heat transfer coefficient (W m^{-2} K^{-1})
h_r: radiative heat transfer coefficient (W m^{-2} K^{-1})
H: convective heat flux (W m^{-2})
H_g: convective heat flux at the globe surface (W m^{-2})
H_{gr}: convective heat flux at the ground surface (W m^{-2})
l: latent heat (J kg^{-1})
L: long-wave radiation flux (W m^{-2})
L_{sky}: long-wave sky radiation flux (W m^{-2})
m: optical air mass
r: radius of the globe (m)
S: short-wave radiation flux (W m^{-2})
S_d: direct solar radiation (W m^{-2})
S_{dif}: diffuse solar radiation (W m^{-2})
S_{nor}: direct solar radiation normal to the beam (W m^{-2})
S_o: global solar radiation (W m^{-2})
S_{po}: solar constant (W m^{-2})
S_{ref}: reflected solar radiation (W m^{-2})
T_a: air temperature (K)
T_g: globe temperature (K)
T_{gr}: ground surface temperature (K)
U: wind speed (m s^{-1})
α_g: absorptivity of the globe for short-wave radiation
β: Bowen ratio
ε_g: emissivity of the globe surface
ε_{gr}: emissivity of the ground surface
θ: solar zenith angle (radian)
σ: Stefan-Boltzmann's constant ($=5.67\times10^{-8}$ W m^{-2} K^{-4})
ρ: air density (kg m^{-3})
τ: atmospheric transmittance

References

Brunt, D., 1939: *Physical and Dynamical Meteorology*. Cambridge University Press, London, 428 pp.

Budd, M., 2008: Wet-bulb globe temperature (WBGT)-its history and its limitations. *J. Sci. Med. Sport*, **11**. 20−32.

Campbell, G. S., and Norman, J. M., 1998: *An Introduction to Environmental Biophysics* (2*nd ed.*). Springer, New York, 286 pp.

Eliasson, I., and Upmains, H., 2000: Nocturnal airflow from urban parks-implications for city ventilation. *Theor. Appl. Climatol.*, **66**(1-2), 95−107.

Gaspar, A. R., and Quintela, D. A., 2009: Physical modelling of globe and natural wet bulb temperatures to predict WBGT heat stress index in outdoor environments. *Int. J. Biometeorol.*, **53**(3), 221−230.

Horie, K., and Fujiwara, H., 2010: Measurement of globe temperature at Sapporo District Meteorological Observatory and trait of the empirical equations to estimate WBGT. *Saihyo*, **56**, 19−21. (in Japanese).

Inoue, K., Nakazono, K., and Kawakata, T., 2004: Numerical experiments for vegetation mitigation effects on thermal environment. *Bull. Natl. Agric. Res. Cent.*, **5**, 1−21. (in Japanese with English abstract).

ISO 7243, 1989: Hot environments-Estimations of the heat stress on working man, based on the WBGT Index (Wet Bulb Globe Temperature). International Standard (1st ed.) International Organization for Standardization (ISO), Geneva.

Japanese Ministry of the Environment, 2011: What is WBGT ? (available at http://www.nies.go.jp /health/HeatStroke/wbgt.html) (in Japanese).

JIS Z 8504, 1999: Hot environments-Estimation of the heat stress on working man, based on the WBGT-index (wet bulb globe temperature). Industrial Standard, Japan Standards Association. (in Japanese).

Kondo, J., 1994: *Hydrometeorology, water and heat budgets on ground surfaces*. Asakura Publishing Co. LTD, Tokyo, 350 pp. (in Japanese).

Kondo, J., 2000: *Atmospheric science near the ground surface*. University of Tokyo Press, Tokyo, 324 pp. (in Japanese).

McAdams, W. H., 1954; *Heat transmission* (3*rd ed.*). McGraw Hill, New York, 249 pp.

Munn, R. E., 1966: Descritive micrometeorology. Academic Press, New York and London, 245 pp.

Murakami, M., and Kimura, F., 2010: anual of handmade field-portable forced ventilation thermometer. *Terr. Environ. Res. Cent. Rep., Univ. Tsukuba*, **11**, 29−33. (in Japanese).

Nagatani, Y., Umeki, K., Honjo, T., Sugawara, H., Narita, K., and Mikami, T., 2008: Analysis of movement of cooled air in Shinjuku gyoen. *J. Agric. Meteorol.*, **64**（4）, 281−288.（in Japanese with English abstract）.

Nakai, S., Yorimoto, A., and Morimoto, T., 1992: The Relation between environmental conditions and the occurrence of exertional heat disorders during physical activity. *Jpn. Soc. Phys. Fit. Sport Med.* **41**（5）, 540−547.（in Japanese with English abstract）.

Ohashi, Y., Ryumon, H., and Shigeta, Y., 2009: Comparison among WBGT values observed at various living and sports spaces in an urban area. *Jpn. J. Biometeorol.* **46**（2）, 59−68.（in Japanese with English abstract）.

Oke, T. R., 1987: Energy and mass exchange. In *Boundary Layer Meteorology*（2*nd ed.*）. Routledge, London, pp. 3−32.

Ono, M., Shimizu, A., and Tsuda, K., 2006: The evaluation of WBGT based on continuous observation. *Jpn. J. Biometeorol.* **43**（3）, S27.（in Japanese）.

Takaichi, M., Hosono, T., Kurosaki, H., Watanabe, S., Kawashima, H., and Nakano, Y., 2003; Estimation of WBGT and evaluation of time and space to work healthily in a greenhouse.（available at http://www.naro.affrc.go.jp/project/results/laboratory/vegetea/2003/vegetea03-24.html）（in Japanese）.

Tonouchi, M., and Murayama, K., 2008: Regional characteristic for the risk of heat attack and HWDI. *Jpn. J. Biometeorol.* **45**（3）, S62（in Japanese）.

Toriyama, A., Monji, N., Aono, Y., and Hamotani, K., 2001: Effects of foliage and sky view factor on the urban thermal environment. *J. Agric. Meteorol.*, **57**（1）, 21−27.（in Japanese with English abstract）.

Yaglou, C. P., and Minard, C. D., 1957: Control of Casualties at Military Training Centers. *Am. Med. Assoc. Arch. Ind. Health*, **16**, 304−314.

Watanabe, K., 1965: *Principles of Architectural Planning*（*Kenchiku-Keikaku Genron*）. Maruzen Co., Tokyo, 240 pp.（in Japanese）.